THE JOURNAL OF BIOLOGICAL CHEMISTRY VOL. 285, NO. 53, pp. 41653–41664, December 31, 2010

Frataxin Depletion in Yeast Triggers Up-regulation of Iron Transport Systems before Affecting Iron-Sulfur Enzyme Activities*

Received for publication, May 28, 2010, and in revised form, October 7, 2010 Published, JBC Papers in Press, October 18, 2010, DOI 10.1074/jbc.M110.149443

Armando Moreno-Cermeño, Èlia Obis, Gemma Bellí, Elisa Cabiscol, Joaquim Ros[1], and Jordi Tamarit

From the Departament de Ciències Mèdiques Bàsiques, Facultat de Medicina, Institut de Recerca Biomèdica de Lleida, Universitat de Lleida, 25008 Lleida, Spain

The primary function of frataxin, a mitochondrial protein involved in iron homeostasis, remains controversial. Using a yeast model of conditional expression of the frataxin homologue *YFH1*, we analyzed the primary effects of *YFH1* depletion. The main conclusion unambiguously points to the up-regulation of iron transport systems as a primary effect of *YFH1* down-regulation. We observed that inactivation of aconitase, an iron-sulfur enzyme, occurs long after the iron uptake system has been activated. Decreased aconitase activity should be considered part of a group of secondary events promoted by iron overloading, which includes decreased superoxide dismutase activity and increased protein carbonyl formation. Impaired manganese uptake, which contributes to superoxide dismutase deficiency, has also been observed in *YFH1*-deficient cells. This low manganese content can be attributed to the down-regulation of the metal ion transporter Smf2. Low Smf2 levels were not observed in *AFT1/YFH1* double mutants, indicating that high iron levels could be responsible for the Smf2 decline. In summary, the results presented here indicate that decreased iron-sulfur enzyme activities in *YFH1*-deficient cells are the consequence of the oxidative stress conditions suffered by these cells.

Frataxin is a small mitochondrial protein that when deficient is the cause of Friedreich ataxia in humans. Homologues of this protein are found in bacteria, fungi, and plants (1). The gene encoding frataxin was identified 14 years ago (2). Initial research performed with yeast cells deficient in the yeast frataxin homologue 1 gene (*YFH1*) indicates the presence of a direct link between frataxin and iron metabolism (3) and the mitochondrial nature of the disease (4, 5). The presence of deficient activities of iron-sulfur-containing enzymes in frataxin- or Yfh1-deficient cells was also observed early and initially considered a consequence of iron-induced oxidative stress (6). A direct role of Yfh1 in iron-sulfur biogenesis was first suggested in 1999 based on the presence of low aconitase activity in yeast Yfh1 mutants grown under iron-limiting conditions (7). Two years later, iron-sulfur deficiency was observed prior to iron accumulation in a conditional frataxin mutant mouse model (8). Both facts support the hypothesis of a primary role for frataxin in iron-sulfur biogenesis, a complex process requiring the participation of several highly conserved proteins called ISC system proteins (9, 10). These proteins are involved in providing the sulfur, iron, and reductive power required to build the cluster. Also, some of them act as scaffold proteins where the newborn clusters are initially accommodated. Finally, a group of proteins participates in the transfer of the cluster from the scaffold proteins to their final host proteins. Many studies have provided evidence that frataxins act as iron donors in iron-sulfur maturation. Most of these studies are based on the finding of direct interactions between frataxins and ISC system proteins such as Isu1 (11–13). However, other findings contradict the hypothesis that frataxin plays a primary role in iron-sulfur biogenesis. For instance, the respiratory function in Yfh1-deficient yeasts can be rescued by limiting iron toxicity, either by expressing human mitochondrial ferritin (14) or overexpressing the vacuolar iron transporter CCC1 (15). Also in yeast, aconitase activity is preserved in Δ*yfh1* cells grown under strict anaerobic conditions (16). Moreover, in two previous studies (17, 18), we observed that *YFH1* null mutations lead to the impairment of superoxide dismutase (SOD)[2] activities. When these activities were restored, the activities of several iron-sulfur-containing enzymes were also recovered, suggesting that iron-sulfur deficiency in Δ*yfh1* yeasts is due to the lack of SOD activities. In frataxin-deficient *Drosophila melanogaster*, aconitase deficiency is observed only under hyperoxia conditions (19), whereas H_2O_2 scavenging restores aconitase activity (20). All of these observations suggest that lack of iron-sulfur enzymatic activities in frataxin-deficient cells could be a consequence of oxidative stress conditions generated by iron accumulation.

The controversy about the primary function of frataxin may be due to the difficulty in differentiating between primary defects directly related to frataxin function and those caused by oxidative stress conditions exerted by iron overload. These latter effects should be considered secondary and not directly related to frataxin function. To solve this problem, some studies have analyzed the evolution of several bio-

* This study was supported by Grants BFU2007-66249/BMC and CSD2007-00020 from the Ministerio de Ciencia e Innovacion and SGR0677 from the Generalitat de Catalunya (Spain).

[1] To whom correspondence should be addressed: Dept. Ciències Mèdiques Bàsiques, Universitat de Lleida, Montserrat Roig, 2, 25008 Lleida, Spain. Tel.: 34-973-702-275; Fax: 34-973-702-426; E-mail: joaquim.ros@cmb.udl.es.

[2] The abbreviations used are: SOD, superoxide dismutase; CBB, Coomassie Brilliant Blue.

TABLE 1
Strains used in this work

Strain	Relevant genotype	Comments
W303-1A	*MAT***a** *ura3-1 leu2-3,112 trp1-1 his3-11,15 ade2-1*	Wild type
W303-1B	*MATα ura3-1 leu2-3,112 trp1-1 his3-11,15 ade2-1*	
MML298	W303-1A *yfh1*::*kanMX4*	Δ*yfh1* (17)
MML348	W303-1A *aft1-Δ5*::*URA3*	Δ*aft1* (45)
BQS100	W303-1A *aft1-Δ5*::*URA3 yfh1*::*kanMX4*	Δ*aft1* Δ*yfh1* (44)
MML830	W303-1A *tetR′-Ssn6*::*LEU2*	Integration of pCM244 in W303-1A (56)
$tetO_2$-YFH1	W303-1A *$tetO_2$-YFH1*::*kanMX4 tetR′-Ssn6*::*LEU2*	Promoter substitution of *YFH1* in MML830
BQS099	W303-1A *$tetO_7$-YFH1*::*kanMX4 tetR′-Ssn6*::*LEU2*	Promoter substitution of *YFH1* in MML830
$tetO_7$-YFH1	W303-1A *$tetO_7$-YFH1*::*kanMX4 tetR′-Ssn6*::*LEU2*	Spore from BQS099 × W303-1B cross
BQS202	*$tetO_2$-YFH1 YFH1-3HA*::*natMX4*	Chromosomal *YFH1* tagged with 3HA using the *natMX4* cassette
BQS203	*$tetO_7$-YFH1; YFH1-3HA*::*natMX4*	Chromosomal *YFH1* tagged with 3HA using the *natMX4* cassette
BQS204	W303-1A *YFH1-3HA*::*natMX4*	Chromosomal *YFH1* tagged with 3HA using the *natMX4* cassette
BQS206	*$tetO_7$-YFH1*; *SMF2-3HA*::*hphNT1*	Chromosomal *SMF2* tagged with 3HA using the *hphNT1* cassette
BQS207	MML298 *SMF2-3HA*::*hphNT1*	Chromosomal *SMF2* tagged with 3HA using the *hphNT1* cassette
BQS208	W303-1A *SMF2-3HA*::*hphNT1*	Chromosomal *SMF2* tagged with 3HA using the *hphNT1* cassette
BQS213	BQS100 *SMF2-3HA*::*hphNT1*	Chromosomal *SMF2* tagged with 3HA using the *hphNT1* cassette
BQS212	MML348 *SMF2-3HA*::*hphNT1*	Chromosomal *SMF2* tagged with 3HA using the *hphNT1* cassette

chemical parameters in frataxin conditional mutants. In yeast, studies taking this approach have used galactose (21)- or methionine (22)-regulated promoters. However, *gal* promoters present the disadvantage of the strong metabolic rearrangements suffered by yeast cells after changes in the carbon source present in the growth media, whereas methionine promoters have not been used to address the early effects of Yfh1 deficiency. An interesting alternative approach was attempted in cell culture using tetracycline-inducible shRNA against frataxin (23). Unfortunately, it is difficult to obtain strong evidence from this model because detailed biochemical analysis of the parameters affected by frataxin depletion in cell lines is very challenging. The present study used yeast *tetO-YFH1* mutants in an effort to decipher the primary consequences of frataxin deficiency. In this model the addition of doxycycline to the growth media allows efficient repression of frataxin expression. This drug is known to have no effects on global expression of the yeast genome (24), avoiding the side effects associated with other kinds of promoters. This approach has allowed us to establish unambiguously that the primary effect of frataxin deficiency is up-regulation of the iron transport systems. We also observed that decreased activities of iron-sulfur-containing enzymes is a secondary effect, resulting from the oxidative stress conditions generated by iron overload and by decreased SOD activities.

EXPERIMENTAL PROCEDURES

Organisms and Culture Conditions—The *Saccharomyces cerevisiae* strains used in this study are listed in Table 1. All of them are derived from W303-1A (*MAT***a** *ura3-1 leu2-3,112 trp1-1 his3-11,15 ade2-1*), which is considered the wild type strain in this work. Yeast cells were grown in rich medium (1% yeast extract and 2% peptone with either 2% glucose (YPD) or 3% glycerol (YPG)) by incubation in a rotary shaker at 30 °C. When indicated, cells were grown in synthetic complete (SC) medium containing 0.67% yeast nitrogen base, a mixture of amino acids, and a carbon source (either 2% glucose or 3% glycerol). All of the experiments described in this work were performed with exponentially growing cells at optical densities ranging from 0.5 to 0.7 (λ = 600 nm, 1-cm light path).

Plasmids and Genetic Methods—The promoter substitution cassettes from plasmids pCM224 and pCM225 were employed for replacing the endogenous promoters of *YFH1* in MML830 by the *$tetO_2$* and *$tetO_7$* promoters as described (25). The primers used for these promoter substitutions were 5′-CAT CGC ACT TGA CAA ATT TCA AAA AAC CGT ATT CAG TGA TCA GCT GAA GCT TCG TAC GC-3′ and 5′-CAC TCT ATC TTC TCG CTT AGT TTT TTT TGA AAT ACT ATC TTT GCA TAG GCC ACT AGT GGA T-3′. Plasmids pCYC106 (supplied by Dr. E. Garí, Universitat de Lleida) and pYM24 (26) were used for 3HA tagging of the coding terminus of the chromosomal copies of *YFH1* and *SMF2*, respectively. The primers used for HA tagging in *YFH1* were 5′-ACT TAC TGA AGA AGT TGA GAA GGC CAT TTC TAA AAG CCA ACG TAC GCT GCA GGT CGA C-3′ and 5′-AAG GAA GAG AGA CTC TAA CTA TGA AAT AGA TTG GAT GCG TCA TCG ATG AAT TCG AGC TCG-3′. The primers used for tagging HA in *SMF2* were 5′-TGA ACT TTT ATA TGT TAC TGG GCT TTA CTA CGG GCA AAG AAG TAC ACC TCC GTA CGC TGC AGG TCG AC-3′ and 5′-ATT CTT GGA TAA AAT GTA TAC TTA TAC TAG TCT AAA GAA TTG TTA TAT TAA TCG ATG AAT TCG AGC TCG-3′. For the overexpression of Mrs4, we used the plasmid JK1489 in which *MRS4* tagged with FLAG at its C terminus was inserted into pCM185 (27), a tetracycline-regulated plasmid. JK1489 was generously supplied by Dr. Jerry Kaplan (University of Utah, Salt Lake City).

Iron and Manganese Analyses—Total cellular iron and manganese concentrations were determined in nitric acid (3%)-digested cells. Cellular volumes were calculated before digestion in a Coulter Z2 particle count and size analyzer. Iron content was determined using bathophenanthroline sulfonate as chelator (28). Manganese content was assayed in a graphite furnace atomic absorption spectrometer.

Enzyme Activities—Cell extracts were prepared using glass beads. Aconitase and citrate synthase enzyme activities were assayed as described (29). SOD activities were analyzed in zymograms. Briefly, cells were disrupted using glass beads in 50 mM Tris-HCl buffer, pH 8.0, and 30 μg of protein were loaded on native Tris-glycine polyacrylamide gels. After electrophoresis, gels were stained for SOD activity as described

(30). Native gels were densitometered in a GS800 densitometer (Bio-Rad), and the density of the bands corresponding to Mn-SOD or CuZn-SOD activity was calculated using Quantity One software (Bio-Rad). A standard curve containing serial dilutions of a reference extract was used to estimate the relative SOD activity in each extract.

Oxygen Consumption—Oxygen consumption was measured in a Clark detector as described (31). In brief, oxygen uptake was measured in a 4-ml stirred chamber (100 rpm) using a YSI model 53 biological oxygen monitor (Yellow Springs Instruments) following the manufacturer's directions. A volume containing 1×10^7 cells grown in YPG was harvested, washed, resuspended in fresh YPG medium and tested for oxygen consumption.

Northern Blot Analyses—RNA isolation and electrophoresis, probe labeling with digoxigenin, hybridization, and signal detection were done as described previously (32). Gene probes were generated by PCR from genomic DNA, using oligonucleotides designed to amplify internal open reading frame sequences.

Western Blot Analysis—Cell extracts were separated in SDS-polyacrylamide gels and transferred to polyvinylidene difluoride (PVDF) membranes. The following primary antibodies were used: Sod2 (Stressgen, SOD-111), Sod1 (Chemicon, AB1237), Aco1 (obtained from R. Lill, Marburg, Germany), Por1 (Molecular Probes, A6449), E2 subunit from α-ketoglutarate dehydrogenase (Kgd2) (33), and antibodies against HA epitope (Roche Applied Science, catalog No. 1867423). Peroxidase-conjugated anti-rabbit and anti-mouse antibodies were used for detection. Image acquisition was performed in a ChemiDoc XRS (Bio-Rad). When required, chemiluminescent data were analyzed using Quantity One software (Bio-Rad). The protein load was verified by post-Western Coomassie Brilliant Blue (CBB) staining of the PVDF membranes.

Carbonyl Quantitation—Oxidative damage to proteins can be evaluated by the use of 2,4-dinitrophenyl hydrazine (DNPH), a compound that reacts with carbonyl groups in proteins. Carbonyl groups are common by-products of oxidative damage to amino acid side chains. Antibodies against DNP allow the immunodetection of this compound bound to proteins by classic Western blot techniques. Crude extracts were prepared as described previously (33). Antibodies against DNP (Dako) were used at a 1:5000 dilution. A peroxidase-conjugated anti-rabbit antibody was used for detection. Images were acquired in a ChemiDoc XRS system (Bio-Rad) and analyzed with Quantity One software (Bio-Rad).

β-Galactosidase Assay—A Fet3-LacZ plasmid containing the FET3 promoter region cloned into YEp354, a LacZ expression vector, was kindly supplied by Dr. Jerry Kaplan (University of Utah) (34). This plasmid was used to transform *tetO*$_7$*-YFH1*cells. Cells were grown in SC medium without the specific marker present in the plasmid. β-Galactosidase activity was measured using a 96-well kinetic assay as described (35). The reaction rate was assayed over a span of 10 min. Specific activity is defined as nmol/min/mg protein.

RNA Isolation and Quantitative Real-time PCR—Total RNA was extracted using the RNeasy kit (Qiagen, catalog no. 74104) according to manufacturer's instructions. 1 μg of total RNA from each sample was converted into cDNA, and 50 ng was used for each individual real-time PCR reaction. The assays were performed in an iCycler (Bio-Rad) using the TaqMan Universal PCR Master Mix kit from Applied Biosystems. Actin (ACT1) was used as an internal control. Primer sequences and probes for *FET3* and *ACT1* were provided by Applied Biosystems (TaqMan gene expression assays, custom). Quantification was completed using iCycler IQ real-time detection system software (version 2.3, Bio-Rad). Relative expression ratios were calculated on the basis of ΔCp values with efficiency correction based on multiple samples (36).

Yeast Cell Fractionation—Mitochondrial and cytosolic fractions were obtained from YPG-grown cells by the following procedure. 0.6 g of yeast cells (wet weight) were resuspended in 2 ml of 100 mM Tris-HCl, pH 9.3, containing 10 mM dithiothreitol and incubated for 30 min at 30 °C. Cells were centrifuged at 1250 × *g* for 4 min, and the pellet was washed with 4 ml of buffer A (25 mM sodium phosphate, pH 7, 1 mM $MgCl_2$, 1 mM EDTA, and 2 M sorbitol). After a second centrifugation step (4 min, 1250 × *g*) the pellet was resuspended in 2 ml of buffer A containing 5000 units of zymolyase. After a 1-h incubation, the spheroplasts were pelleted by centrifugation at 2800 × *g* for 7 min. The pellet was resuspended in 2 ml of 10 mM Tris-HCl, pH 7.4, containing 1 mM EGTA, 0,32 M sucrose, and protease inhibitors. The spheroplast suspension was subjected three times to 10 strokes in a cooled Potter-Elvehjem tissue grinder (Kimble/Kontes) and centrifuged at 1250 × *g* for 4 min to eliminate unbroken cells and debris. The supernatant was centrifuged again (10 min, 7800 × *g*) to separate the cytosolic proteins (which remained in the supernatant) from the mitochondria pellet.

Immunoprecipitation of Yfh1—Mitochondrial or cytoplasmic proteins (200 μg) were immunoprecipitated using a μMACS^{TM} column (Miltenyi Biotec) prepared for HA-tagged protein isolation according to manufacturer's instructions. The immunoprecipitated proteins were separated by SDS-PAGE, blotted onto nitrocellulose membranes, and inmunodetected using anti-HA antibodies.

Measurement of Cell Growth Rate—Cell growth was monitored in 1-ml cultures in 24-well plates incubated at 30 °C and constant agitation in a Biotek PowerWave XS Microplate Spectrophotometer. Plates were sealed with Breathe-EASY membranes (Diversified Biotech, Boston, MA). Optical density (600 nm) was recorded every 30 min. Generation times were calculated every hour using four measurements around the desired time point. Gen5 data analysis software and Microsoft Excel were used for these calculations.

RESULTS

Selection of Growth Media—The present study used yeast *tetO-YFH1* mutant strains in which the endogenous *YFH1* gene was placed under the control of a Tet promoter. Nevertheless, we first analyzed the effect of the growth media on mitochondrial content and activity in our wild type strain (W303-1A) to select the optimal growth conditions for this study. Glucose is the preferred carbon source of *S. cerevisiae*,

and consequently this sugar exerts a strong repressive effect over many genes involved in the utilization of other carbon sources. Glucose also has a strong repressive effect on many mitochondrial genes involved in respiration or NADH generation. As a consequence, yeast grown under conventional YPD medium (which contain 2% glucose) display a respirofermentative metabolism in which most of the glucose used is converted to ethanol. This phenomenon is known as the Crabtree effect (37, 38). Yeast cells can also grow efficiently in rich medium containing glycerol (YPG), which is a nonfermentable carbon source. Therefore, we analyzed several mitochondrial markers, both in YPD- and YPG-grown cells, including two enzymatic activities (aconitase and mitochondrial citrate synthase) and three proteins (aconitase, α-ketoglutarate dehydrogenase, and the mitochondrial porin). As shown in Fig. 1, all of these parameters were higher in cells grown in YPG, indicating strong repression of mitochondrial function in cells grown in YPD medium. As a result, YPG medium was selected to perform our experiments. It is worth reminding that frataxin is a mitochondrial protein, and tissues most affected in Friedreich ataxia are those with high oxygen consumption (39).

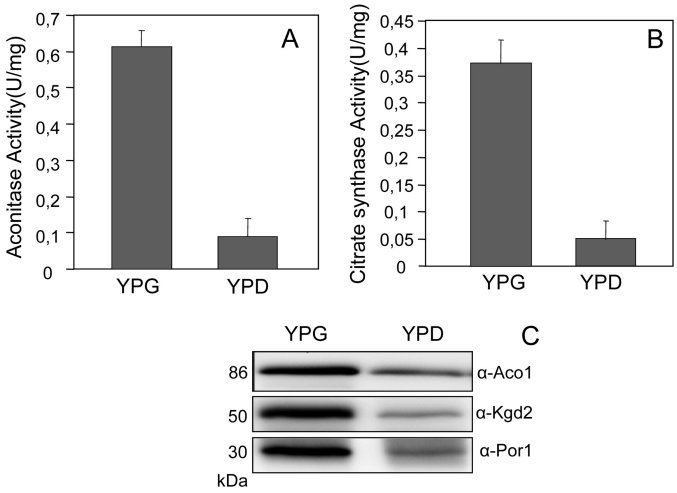

FIGURE 1. **Increased mitochondrial content in YPG-grown cells.** W303 cells were grown in either YPG or YPD medium. Enzymatic activities of aconitase (*A*) and citrate synthase (*B*) were measured in whole cell extracts. The protein content of Aco1, Kgd2, and Por1 was analyzed using specific antibodies (*C*). In each gel lane, 15 μg of protein from whole cell extracts was loaded. The protein load was also verified by post-Western CBB staining of the PVDF membrane. The apparent molecular weight of each protein is shown in kDa.

Construction and Validation of Conditional YFH1 Mutant Strains—We constructed two conditional mutants in which *YFH1* expression was placed under the control of either $tetO_2$ *or* $tetO_7$ promoters. For this purpose, we generated $tetO_2$-*YFH1* and $tetO_7$-*YFH1* strains in which the wild type *YFH1* promoter was replaced by these two promoters. Because these promoters differ in the number of activation/repression boxes they contain, $tetO_7$ promoters are more efficient than $tetO_2$ promoters (32). Both of the *tetO-YFH1* strains were able to grow on glycerol in the absence of doxycycline (*YFH1* expressed). The level of expression of *YFH1* was measured by Northern blot before and after 7 h of exposure to doxycycline (Fig. 2*A*). Wild type and Δ*yfh1* strains were used as controls. As expected, $tetO_7$-*YFH1* presented higher levels of expression than $tetO_2$-*YFH1* in the absence of doxycycline, whereas in the presence of this drug the repression was stronger in $tetO_7$-*YFH1* than in $tetO_2$-*YFH1*. To evaluate the effect of the different expression levels on protein levels, a 3× HA tag was placed at the C-terminal site of Yfh1 in wild type and *tetO-*

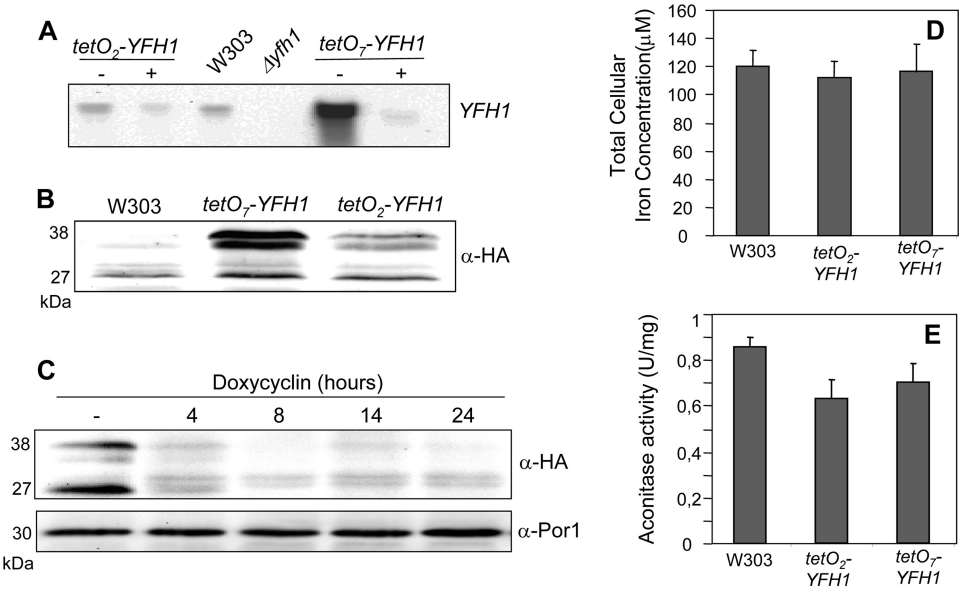

FIGURE 2. **Validation of conditional *YFH1* mutant strains.** *A*, W303, $tetO_2$-*YFH1*, and $tetO_7$-*YFH1* cells were grown in YPD medium, and the expression of *YFH1* was analyzed by Northern blot before and after the addition of doxycycline (7 h) to the growth medium. *B*, the effect of the promoter on Yfh1 protein levels was analyzed in YPG-grown cells by Western blot in the HA-tagged versions of the described strains. *C*, evolution of Yfh1-HA and Por1 protein content after doxycycline addition in the $tetO_7$-*YFH1-HA* strain grown in YPG medium. The detectable signal in the α-HA Western blot after 8 h of doxycycline addition corresponds to a nonspecific signal. In *B* and *C*, 30 μg of protein from whole cell extracts was loaded in each gel lane, and the protein load was verified by post-Western CBB staining of the PVDF membrane. *D*, total cellular iron concentration was quantified in YPG-grown cells as described under "Experimental Procedures." *E*, aconitase activity was measured in whole cell extracts from YPG-grown cells. Data are representative of means ± S.D. from three independent experiments. The apparent molecular weight of each protein is shown in kDa.

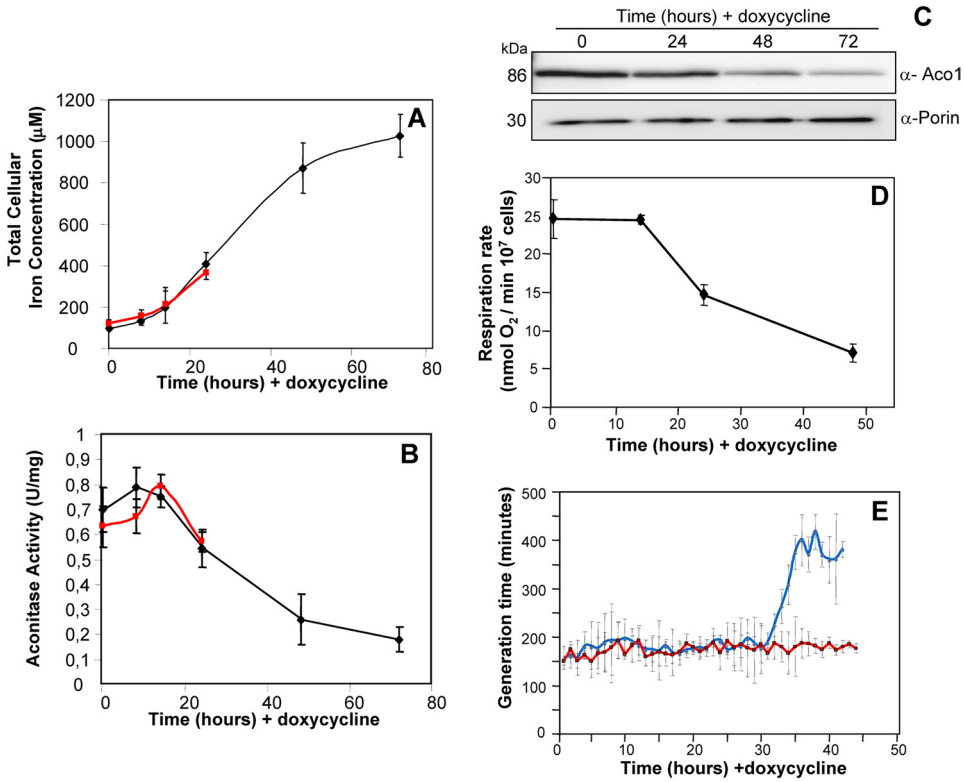

FIGURE 3. **Evolution of aconitase activity and iron content after Yfh1 depletion.** Total cellular iron concentration (*A*) and aconitase activity (*B*) were measured in YPG-grown *tetO*$_2$*-YFH1* (*red line*) and *tetO*$_7$*-YFH1* cells (*black line*) after doxycycline addition. *C*, Aco1 and Por1 protein content was measured in YPG-grown *tetO*$_7$*-YFH1* cells using specific antibodies. In each gel lane, 15 μg of protein from whole cell extracts was loaded, and protein load was verified by post-Western CBB staining of the PVDF membrane. The apparent molecular weight of each protein is shown in kDa. *D*, oxygen consumption (nmol O_2 min^{-1}) was measured by a Clark-type electrode. Data are representative of means ± S.D. of three independent experiments. *E*, *tetO*$_7$*-YFH1* cells were grown in 24-well plates in YPG medium containing (*blue line*) or not containing (*red line*) 2 μg/ml doxycycline. Generation time was calculated for each condition as explained under "Experimental Procedures." Data are representative of mean ± confidence intervals from five independent cultures.

regulated strains. Western blot analysis revealed the presence of three bands (Fig. 2*B*). The fast migrating band corresponds to the mature form of the protein, whereas bands of higher molecular weight correspond to the immature forms. Wild type and *tetO*$_2$*-YFH1-HA* presented similar levels of the mature form, whereas some increase in this form could be observed in the *tetO*$_7$*-YFH1-HA* strain. Immature forms where found increased in both of the conditional strains, although this increase was higher in the *tetO*$_7$*-YFH1-HA* strain. After doxycycline addition (Fig. 2*C*), both the mature and immature forms disappeared, and the Yfh1 signal was undetectable after 8 h of incubation with the drug. As an additional control, we analyzed the iron levels and aconitase activity in the different strains used. As shown in Fig. 2, *D* and *E*, no relevant changes were observed in these parameters between the different strains. Finally, we analyzed the effects of doxycycline addition to the wild type strain on iron levels, aconitase activity, and SOD amounts (measured by Western blot). No significant changes were observed in any of these parameters after 24 h of incubation with doxycycline (not shown). This observation is consistent with previous reports indicating no doxycycline effect on global gene expression in *S. cerevisiae* (24). All of these data indicate that neither the substitution of the *YFH1* promoter nor the addition of doxycycline *per se* has a major effect on the parameters under study. Therefore, any effect observed on the conditional mutants after doxycycline addition may be attributed to Yfh1 depletion.

Analysis of Iron Accumulation and Aconitase Activity on the Conditional Mutants—We analyzed the effect of doxycycline addition on total cellular iron content and aconitase activity in both strains: *tetO*$_2$*-YFH1* at 0, 8, 14 and 24 h and *tetO*$_7$*-YFH1* at 0, 8, 14, 24, 48, and 72 h. Iron accumulation was detected after 14 h of *YFH1* repression in both strains, reaching a 10-fold increase after 72 h of doxycycline addition in *tetO*$_7$*-YFH1* (Fig. 3*A*). Aconitase activity (Fig. 3*B*) was stable for 14 h and then slowly began to decrease after 24 h of incubation. After 72 h, less than 30% of the initial activity could be detected. Western blot analysis of Aco1 protein content (Fig. 3*C*) indicated that decreased aconitase activity was due to the loss of Aco1 protein. Mitochondrial porin was used as a control of mitochondrial content. This protein remained constant throughout the incubation, indicating that the observed decrease in aconitase activity and content was not due to a general loss of mitochondria. During the first 24 h of *YFH1* repression, the patterns of iron accumulation and aconitase activity were similar in both *tetO*$_2$*-YFH1* and *tetO*$_7$*-YFH1* strains, indicating that the original levels of Yfh1 do not have a marked effect on the evolution of the parameters analyzed.

Decline in Respiratory Function—Respiratory failure is a common trait in Yfh1-deficient cells. This failure may result from inactivation of several iron-sulfur-containing proteins, including aconitase and those present in the mitochondrial complexes of the respiratory chain. As a measure of respiratory function, oxygen consumption was analyzed in *tetO*$_7$-

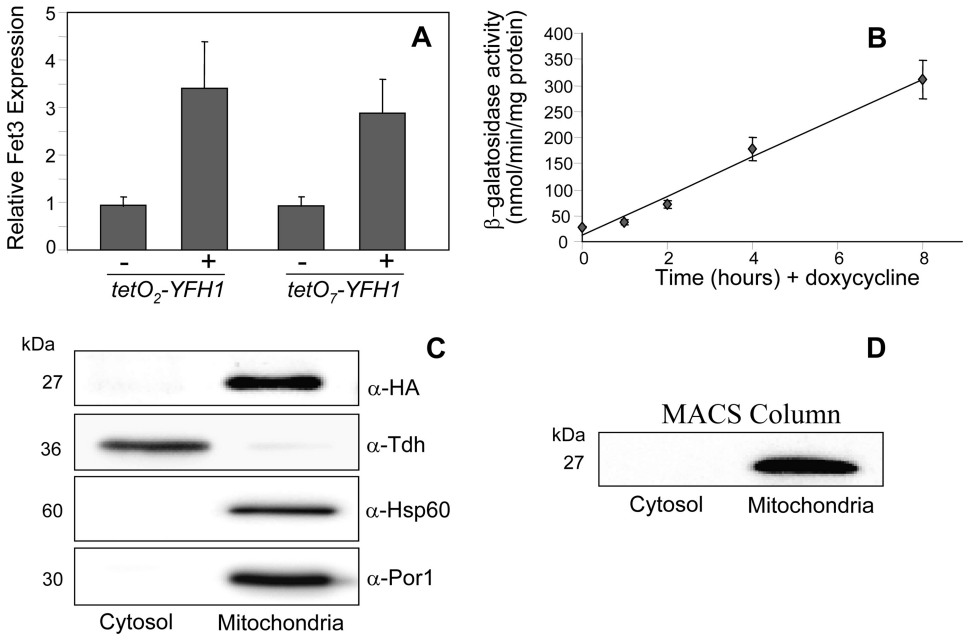

FIGURE 4. **Early induction of Fet3 after Yfh1 depletion.** *A*, relative expression of *FET3* in the indicated strains was analyzed in YPG-grown cells before (−) and after 4 h of addition of doxycycline (+) by quantitative RT-PCR. Reference values are those observed in untreated *tetO$_2$-YFH1* cells. *ACT1* was used as a control. *B*, *tetO$_7$-YFH1* cells transformed with a plasmid containing a FET3-LacZ construction were grown in SC medium plus glycerol, and β-galactosidase activity was measured at the indicated time points after doxycycline addition. In both panels, Data are representative of means ± S.D. from three independent experiments. *C*, mitochondrial and cytosolic fractions were prepared from YPG-grown BQS204 cells (as described under "Experimental Procedures") and loaded on SDS-polyacrylamide gels. The indicated proteins were detected by Western blot. *D*, mitochondrial and cytosolic fractions were subjected to immunoprecipitation using antibodies against the HA tag and MACS magnetic beads. The immunoprecipitate was loaded on SDS- polyacrylamide gels and analyzed for the presence of Yfh1-HA using antibodies against this tag. The apparent molecular weight of each protein is shown in kDa.

YFH1 cells using a Clark-type electrode. As shown in Fig. 3*D*, oxygen consumption remained constant in our conditional model during the first 14 h after doxycycline addition followed by a progressive decline. This pattern indicates that, similar to aconitase, iron-sulfur centers in respiratory chain complexes were not quickly affected by Yfh1 depletion.

Decline in Growth Rate—We followed the effect of Yfh1 depletion on the growth rate of the tetO$_7$-*YFH1* strain. We performed these experiments in 24-well plates containing 1 ml of YPG cultures. These plates, containing control cells and doxycycline-treated cells, were incubated in a Biotek PowerWave XS Microplate Spectrophotometer. As described under "Experimental Procedures," cultures were kept at log phase by diluting in a new plate every 12 h. Optical density was measured every 30 min, and generation times were calculated for each culture considering 2-h time lapses. As shown in Fig. 3*E*, a significant increase in the generation time was observed after 30 h of treatment with doxycycline. Notably, this increase parallels with the loss in aconitase activity and respiratory function described above.

Activation of the Iron Regulon Precedes Aconitase Inactivation—The results presented above suggest that iron accumulation precedes the decline in aconitase activity and oxygen consumption as observed, for instance, after 24 h of incubation with doxycycline. At this time point, total cellular iron has increased nearly 4 times, both in *tetO$_2$-YFH1* and *tetO$_7$-YFH1* strains, whereas aconitase activity presents only a slight (10%) and insignificant decrease (Fig. 3, *A* and *B*). This finding suggests that Aft1p, the transcription factor involved in iron homeostasis, is activated early, before aconitase activity or oxygen consumption decrease. This finding is highly relevant, because most authors consider iron accumulation in Δ*yfh1* strains to be one of the consequences of iron-sulfur deficiency, as Aft1p is known to be activated by the disruption of iron-sulfur biogenesis (40). However, if this canonical hypothesis were true, our conditional model would show a decrease in aconitase activity before Aft1p activation. To further confirm the early activation of iron-responsive genes after Yfh1p depletion, we measured the expression of *FET3* by quantitative RT-PCR at 4 h after doxycycline addition in both the *tetO$_2$-YFH1* and *tetO$_7$-YFH1* strains. The Fet3 protein plays a central role in the high affinity iron transport system of yeast and is strongly induced after Aft1 activation (41). The results presented in Fig. 4*A* indicate a clear induction of the *FET3* transcript in both strains. To further investigate this point, we transformed the *tetO$_7$-YFH1* strain with a plasmid containing a LacZ reporter gene under the control of the Fet3 promoter. Fig. 4*B* shows the evolution of LacZ activity in the transformed strain after addition of doxycycline. A progressive increase in LacZ activity was observed soon after doxycycline addition, confirming the quantitative RT-PCR data. In summary, our data indicate that induction of the high affinity iron transport system in the absence of Yfh1 is not triggered by a general decrease in iron-sulfur centers, thus questioning the idea that iron-sulfur biogenesis is a primary function of frataxin or Yfh1.

Absence of Extramitochondrial Yfh1—The results described above indicate that depletion of Yfh1 leads to an early activation of the high affinity iron transport system through an unknown mechanism not dependent on iron-sulfur biosynthesis.

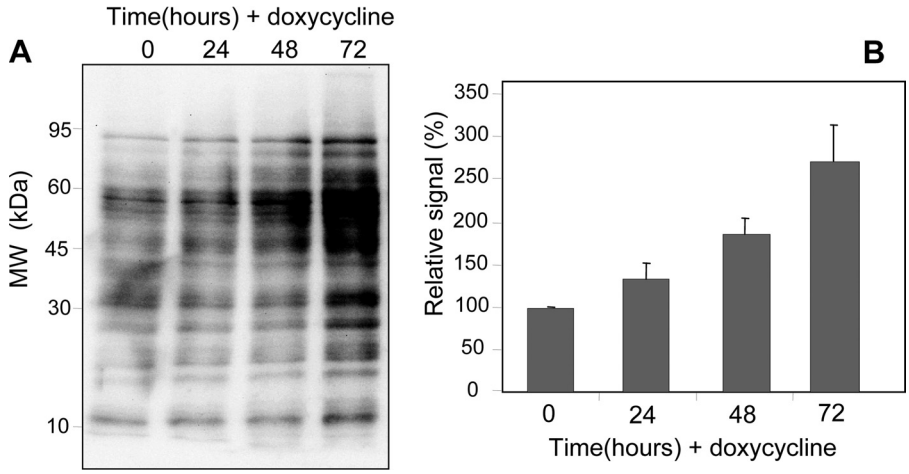

FIGURE 5. **Oxidative damage as carbonylation increases after Yfh1 depletion.** *A*, carbonylated proteins were detected by Western blot using α-DNP antibodies at the indicated time points after doxycycline addition in YPG-grown *tetO$_7$-YFH1* cells. *B*, the chemiluminescent signal of each lane of the Western blot was analyzed using Quantity One software (Bio-Rad). Carbonyl levels at time point 0 were used as the 100% reference. Data are representative of means ± S.D. from three independent experiments.

We wanted to explore the presence of a cytosolic form of Yfh1 that could act as a regulator of Aft1. In human cells, the presence of an extramitochondrial form of frataxin has been reported that could be involved in IRP1 regulation (42). It should be noted, however, that the existence of such an extramitochondrial form of frataxin has been questioned by other authors (43). To analyze the existence of such an extramitochondrial form of Yfh1, yeast cells carrying an HA-tagged Yfh1 (strain BQS204) were fractionated and analyzed by Western blot for the presence of Yfh1-HA in the cytosolic and mitochondrial fractions (Fig. 4*C*). The mitochondrial proteins Hsp60 and Por1 were not detected in the cytosolic fraction, indicating the absence of mitochondrial contamination in such fractions. The cytosolic protein glyceraldehyde-3-phosphate dehydrogenase (Tdh1) was used as a cytosolic marker. The presence of Yfh1-HA could not be detected in the cytosolic fraction. This may be due to the presence of minute amounts of Yfh1, not detectable by Western blot, a technique with a limited dynamic range. To overcome this limitation and further confirm the absence of Yfh1 in the cytosol, we immunoprecipitated this protein in the cytosolic and mitochondrial fractions using anti-HA antibodies. Again, Yfh1-HA could not be detected in the cytosolic fraction (Fig. 4*D*). These results suggest that yeast cells do not display a cytosolic form of Yfh1. Activation of the high affinity iron transport system in *YFH1*-deficient cells may then be triggered by mitochondrial events.

Protein Oxidative Damage—Oxidative stress could explain the progressive decrease of aconitase protein and activity in *tetO$_7$-YFH1* after doxycycline addition. Iron overload is known to trigger oxidative stress, which would compromise the activity of aconitase, a protein highly sensitive to such stress. We decided to analyze the presence of protein carbonylation, a known marker of protein oxidative damage, in *tetO$_7$-YFH1* after doxycycline addition. Carbonyl groups are common by-products of the free radical attack on amino acid side chains. They can be detected by Western blot after derivatization with DNPH (33). Protein carbonylation has been found previously to be increased in Δ*yfh1* mutants (16, 44) as well as in other mutants showing iron accumulation (45). Fig. 5 shows the progressive accumulation of carbonyl groups on proteins after Yfh1 depletion in the *tetO$_7$-YFH1* strain. Analysis of the chemiluminescent data reveals a significant increase in protein carbonylation after 24 h of incubation with doxycycline, indicating the presence of a strong oxidative environment under such conditions. This could explain the observed decline in aconitase at this same time point.

Evolution of SOD Amounts and Activities—In two previous studies, we showed that SODs play a central role in protein oxidative damage in null *YFH1* yeast cells. First, we observed the presence of decreased Mn-SOD activity in Δ*yfh1*, which compromise the activity of some iron-sulfur-containing enzymes (17). We also observed that decreased activities of SOD1 and SOD2 contribute to oxidative damage to a specific subset of proteins by increasing the presence of chelatable iron in Δ*yfh1* cells (18). We wanted now to explore the evolution of both SOD enzymes on the conditional *tetO-YFH1* strains and their potential relevance to aconitase deficiency. To this purpose we analyzed changes in protein content (by Western blot) and enzymatic activities (by zymograms) of both SOD isoenzymes after doxycycline addition to the growth media. Again, *tetO$_2$-YFH1* was monitored for 24 h and *tetO$_7$-YFH1* for 72 h. SOD protein amounts were induced progressively after Yfh1 repression in both strains (Fig. 6*A*). This induction was also observed previously in Δ*yfh1* mutants (17, 44) and may be the consequence of the oxidative stress conditions exerted by iron overload. Enzymatic activities were measured using zymograms, which allow a clear differentiation of both isoenzymes (Fig. 6*B*). As shown in Fig. 6, *C* and *D*, enzymatic activities did not correlate to protein amounts (Fig. 6*A*) over the time course of the study. Mn-SOD activity decreased steadily over the time course of the study, whereas CuZn-SOD showed an initial increase followed by a progressive decline after 24 h of incubation with doxycycline.

Evolution of Manganese and Smf2 Levels—We were interested in understanding the origin of the Mn-SOD activity de-

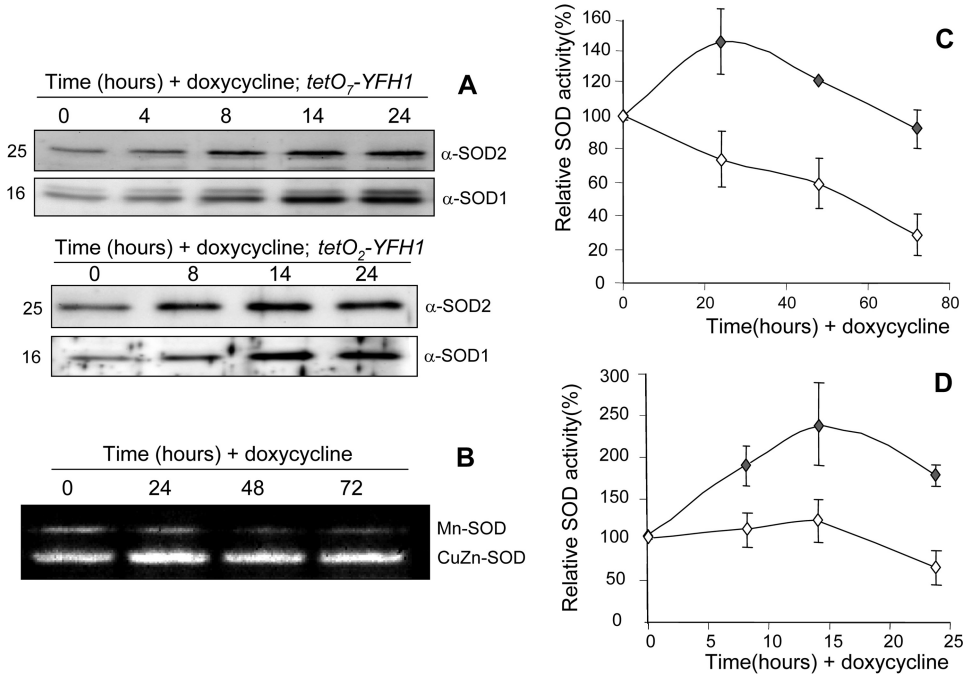

FIGURE 6. **Evolution of SOD content and activity after Yfh1 depletion.** *A*, evolution of Sod1 and Sod2 protein content in the indicated strains after the addition of doxycycline was analyzed by Western blot using specific antibodies. In each gel lane, 15 μg of protein from whole cell extracts was loaded, and protein load was verified by post-Western CBB staining of the PVDF membrane. The apparent molecular weight of each protein is shown in kDa. *B*, a representative zymogram from *tetO*$_7$*-YFH1* is shown, with the *bands* corresponding to Mn-SOD and CuZn-SOD activity indicated. *C* and *D*, CuZn SOD activity (*gray rhombus*) and Mn-SOD activity (*white rhombus*) were measured by zymograms in YPG-grown *tetO*$_7$*-YFH1* (*C*) and *tetO*$_2$*-YFH1* cells (*D*) at different time points after doxycycline addition. Activities at time point 0 were used as 100% reference. Data are representative of means ± S.D. from three independent experiments.

ficiency in Yfh1-deficient cells. Previously, we reported that Δ*yfh1* mutants exhibited decreased total cellular manganese content. Manganese supplementation of the growth media restored normal manganese levels and recovered Mn-SOD activity, suggesting that inactivation of Mn-SOD was due to limited cofactor availability (17). The reasons for this manganese deficiency in Δ*yfh1* cells and their relationship with Yfh1 were not investigated. Therefore, we analyzed the manganese content at 0, 24, 48, and 72 h of incubation with doxycycline in the *tetO*$_7$*-YFH1* strain and observed a decline on this metal content after 48 h (Fig. 7*A*). This is consistent with previous observations in the null mutant and suggests that manganese deficiency is a late effect of Yfh1 depletion not directly linked with the primary function of Yfh1. To analyze the possibility of an early deficiency of this metal in mitochondria, manganese content was also measured in mitochondrial fractions after 24 h of doxycycline addition. No significant differences were found in the manganese content in this organelle at this time point (data not shown). To find the reason for the total cellular manganese content deficiency, we decided to analyze the expression of Smf2, an internal membrane protein required for manganese uptake. Loss of this protein leads to decreased manganese cellular content and decreased Mn-SOD activity, which can be recovered by manganese supplementation of the growth media (46). Smf2 is regulated at the post-translational level by iron and manganese levels. Upon metal-replete conditions, it is targeted to the vacuole for degradation (47). By Western blot, we followed the presence of Smf2 after doxycycline addition to BQS206, a *tetO*$_7$*-YFH1* strain with a HA-tagged version of Smf2. We observed a progressive decline of Smf2 levels after 14 h of incubation (Fig. 7, *B* and *C*), which became more marked after 48 h of incubation when only 40% of the original levels of the protein could be detected. Thus, manganese deficiency in Yfh1-depleted cells may be due to the loss of this protein. To further understand the Smf2 deficiency, we investigated the presence of Smf2-HA in Δ*yfh1*, Δ*aft1*, and double Δ*yfh1*Δ*aft1* strains. Mutation of *AFT1* prevents iron accumulation in a Δ*yfh1* background (44). As shown in Fig. 7*D*, Smf2 levels are very low in Δ*yfh1* in contrast to the levels observed in Δ*aft1* and in the double Δ*yfh1*Δ*aft1* mutants. This suggests that decreased Smf2 levels in both Δ*yfh1* and *tetO*$_7$*-YFH1* are due to iron accumulation. In contrast to Aft1, Smf2 could be able to sense increased iron levels in Δ*yfh1* cells and lead to decreased high affinity manganese transport.

Effect of Manganese Supplementation on SOD and Aconitase—In a previous study in Δ*yfh1* cells (17), we observed protection of several iron-sulfur enzymes by manganese supplementation of the growth media. This treatment also restored Mn-SOD activity. This finding suggested that iron-sulfur enzymes are inactivated by the oxidative stress conditions created by decreased Mn-SOD activity and iron overload. However, manganese treatment in Δ*yfh1* cells was unable to restore aconitase activity. This differential behavior of aconitase could be due merely to increased sensitivity of this enzyme toward oxidative stress (relative to the other iron-sulfur enzymes tested), or to the existence of a specific role of Yfh1 in holo-aconitase maturation or stability. The conditional *tetO*$_7$*-YFH1* model used in this work allowed us to better address the relationship between decreased SOD and

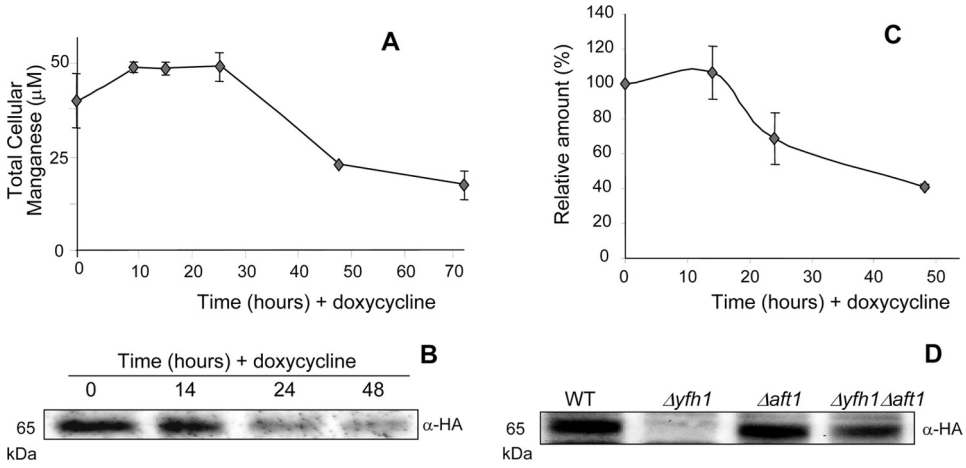

FIGURE 7. **Total cellular manganese and Smf2 levels in Yfh1-depleted cells.** *A*, evolution of total cellular manganese concentration was analyzed in YPG-grown *tetO$_7$-YFH1* cells after doxycycline addition. *B*, analysis by Western blot of the content, after doxycycline addition, of an HA-tagged version of Smf2 in a *tetO$_7$-YFH1* strain (BQS206). In each gel lane, 30 μg of proteins from whole cell extracts was loaded, and protein load was verified by post-Western CBB staining of the PVDF membrane. *Wt*, wild type. *C*, to calculate the Smf2 relative content at the indicated time points, the chemiluminescent signal from each lane of the Western blot was analyzed using Quantity One software (Bio-Rad). Smf2-HA levels at time point 0 were used as the 100% reference. *D*, analysis by Western blot of Smf2-HA content in strains presenting the indicated mutations. In each gel lane, 30 μg of protein from whole cell extracts was loaded, and protein load was verified by post-Western CBB staining of the PVDF membrane. In all panels, Data are representative of means ± S.D. from three independent experiments. The apparent molecular weight of each protein is shown in kDa.

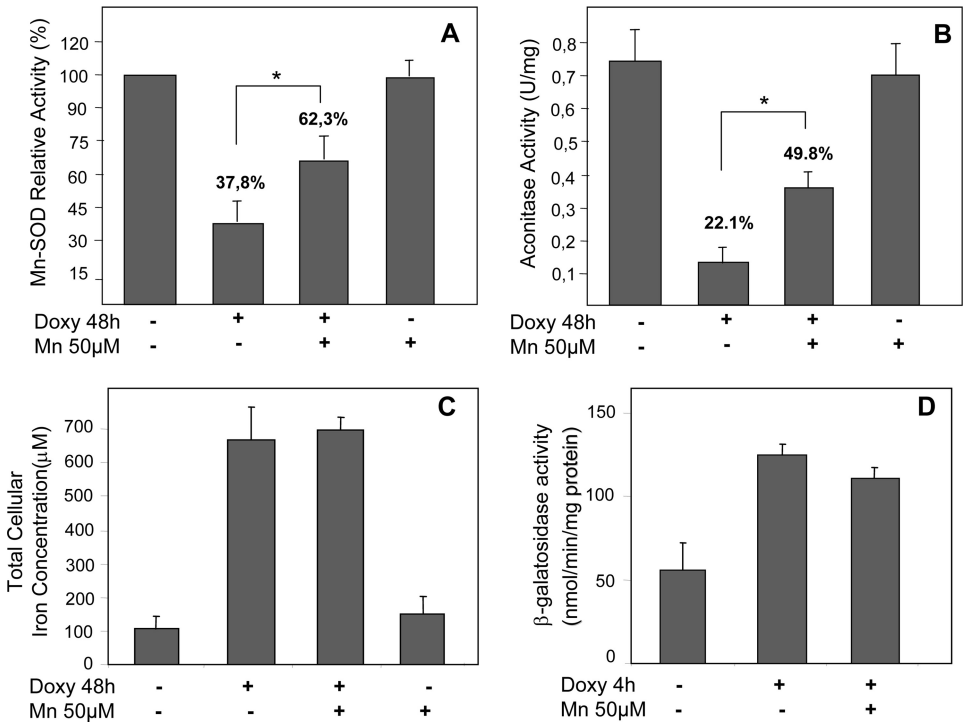

FIGURE 8. **Manganese treatment prevents the decline in Mn-SOD and aconitase activities.** *A–C*, the enzymatic activities of Mn-SOD (*A*), aconitase (*B*), and total cellular iron were measured in YPG-grown *tetO$_7$-YFH1* cells exposed (+) or not (−) to doxycycline (*Doxy*) and 50 μM $MnCl_2$ for 48 h. For Mn-SOD, the values of the nontreated cells were used as the 100% reference. Manganese treatment provided a significant protection to both enzymatic activities (*, $p < 0.05$). *D*, *tetO$_7$-YFH1* cells transformed with a plasmid containing a FET3-LacZ construction were grown in SC-glycerol medium supplemented (+) or not (−) with 50 μM $MnCl_2$. β-Galactosidase activity was measured 4 h after doxycycline addition. Data are representative of means ± S.D. from three independent experiments.

aconitase activities. The results presented in Figs. 3 and 6 indicate that both Mn-SOD and aconitase activities showed a similar inactivation rate, suggesting that aconitase inactivation could be triggered by a decrease in Mn-SOD activity. To confirm this triggering, we analyzed the effect of manganese supplementation on Mn-SOD and aconitase activities in the conditional *tetO$_7$-YFH1* mutant. We measured both activities in cultures treated with doxycycline for 48 h and supplemented or not with 50 μM manganese. As shown in Fig. 8, *A* and *B*, manganese had a similar protective effect on both aconitase and Mn-SOD activities in the doxycycline-treated cells (Yfh1 OFF), whereas no effect of this metal was observed in the control cultures not treated with doxycycline (Yfh1 ON). These data support the hypothesis that aconitase inacti-

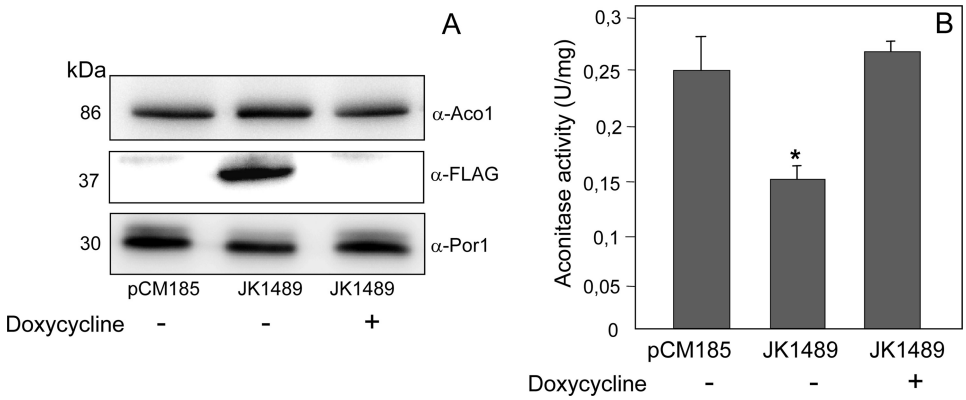

FIGURE 9. **Overexpression of MRS4 promotes inactivation of aconitase.** W303 cells were transformed with plasmid JK1489 (containing *MRS4* tagged with FLAG) or with the plasmid vector (pCM185). Cells were grown in SC-glucose medium. Where indicated, doxycycline was added at 2 μg/ml. *A*, aconitase, Mrs4-FLAG, and porin were detected by Western blot using the indicated antibodies. In each gel lane, 15 μg of protein from whole cell extracts was loaded, and protein load was verified by post-Western CBB staining of the PVDF membrane. The apparent molecular weight of each protein is shown in kDa. *B*, aconitase activity was measured in whole cell extracts. A significant decrease in aconitase activity was found in the cells overexpressing Mrs4 (*, $p < 0.05$). Data are representative of means ± S.D. from three independent experiments.

vation may be triggered by increased superoxide levels due to decreased Mn-SOD activity. As a control, total cellular iron content was measured after 48 h of treatment, and Fet3 promoter activity was measured after 4 h of doxycycline addition (using the Fet3LacZ construction). As shown in Fig. 8, *C* and *D*, neither of these parameters was affected by manganese supplementation.

Effect of Mitochondrial Iron Overload on Aconitase—To confirm the sensitivity of aconitase under iron overload conditions, we transformed wild type yeast cells with a multicopy plasmid carrying a FLAG-tagged version of the mitochondrial iron transporter Mrs4 under a *tet*-regulated promoter. This led to overexpression of this transporter (Fig. 9*A*), which promotes mitochondrial iron overload (48). As shown in Fig. 9*B*, such overexpression resulted in a 50% decrease in aconitase activity. When expression of Mrs4 was repressed by the addition of doxycycline (or in cells transformed with the void plasmid) this inactivation was not observed. This result indicates that excess iron in the mitochondria contributes to aconitase inactivation.

DISCUSSION

Fourteen years after the discovery of the gene coding for frataxin, the precise function of this protein remains a matter of debate. According to the results shown here, the primary role of frataxin in iron-sulfur biogenesis should be questioned. The use of conditional Yfh1 mutants in this work has allowed us to overcome one of the main difficulties in analyzing the effects of frataxin deficiency: distinguishing primary defects directly due to the absence of the protein from those defects due to oxidative stress exerted by iron deregulation. Our results indicate that deregulation of iron metabolism is the primary effect of Yfh1 depletion, as increased expression of Fet3 was clearly observed 4 h after doxycycline addition in both $tetO_2$-*YFH1* and $tetO_7$-*YFH1* strains. This induction was observed by quantitative RT-PCR analysis, as well as with the Fet3-LacZ reporter protein. Iron accumulation was also observed at the early stages of Yfh1 depletion. The remaining effects (increased protein oxidative damage, decreased aconitase and SOD activities, decreased oxygen consumption, and decreased manganese and Smf2 levels) were observed only after 24 or 48 h of doxycycline addition. Therefore, all of these may be secondary effects, the consequence of iron overload.

The more controversial point in this hypothesis is the understanding of the mechanism that explains aconitase deficiency in Yfh1-depleted cells. This deficiency cannot be primary, as most of the activity of this enzyme remained stable 24 h after doxycycline addition, whereas iron overload, protein oxidative damage, and induction of both SOD isoenzymes were clearly observed at this time point. Previous observations indicate that disruption of genes involved in iron-sulfur biogenesis leads to a rapid loss in aconitase activity. Reduction of *GRX5* expression through the use of a *tet*-regulated promoter leads to a more than 80% decrease in aconitase activity within 12 h (45). Such a rapid decrease has also been observed in a Met-regulated Nfs1 strain (40). Both observations suggest that aconitase does not present a long half-life. Also, as yeast cells are not arrested during the first 24 h of treatment, the remaining aconitase activity cannot be attributed to the initial holo-aconitase pool. Indeed, the presence of high aconitase activity at this time point indicates that the biochemical machinery required for holo-aconitase maturation remains active in the absence of Yfh1. Aconitase activity decline appears to be a consequence of oxidative stress. First, markers of oxidative stress, such as carbonyl content or Sod1p and Sod2p content, were found increased at 24 h after doxycycline addition. Second, mitochondrial Mn-SOD activity was also decreased after 48 h of incubation. The presence of decreased activities of iron-sulfur enzymes has been widely described in different organisms as one of the consequences of decreased SOD activity, as this type of cofactor is extremely sensitive to superoxide (49). Finally, when inactivation of Mn-SOD activity is prevented by manganese supplementation of the growth media, a decline in aconitase activity was also prevented. This last observation highlights the relationship between decreased Mn-SOD and aconitase activities, previously analyzed in Δ*yfh1* cells (17, 18). Under such conditions, re-

storing Mn-SOD activity prevented inactivation of three iron-sulfur-containing enzymes (succinate dehydrogenase, glutamate synthase, and isopropyl malate dehydrogenase) but not of aconitase. The present work indicates that this difference between aconitase and other iron-sulfur-containing enzymes may be due to the increased sensitivity of aconitase toward oxidative stress conditions.

Iron overload may trigger the deficiencies observed in manganese and SOD activities. These anomalies were observed previously and investigated in Δ*yfh1* mutants (17, 18). Mn-SOD deficiency was considered the consequence of an imbalance between reduced cofactor (manganese) levels and increased iron content that would promote the accumulation of apo-Sod2 and Fe-Sod2, two inactive forms of the enzyme. However, the origin of manganese deficiency was not completely understood. In this work, we observed a decline in Smf2, a protein involved in manganese uptake, both in Δ*yfh1* cells and in *tetO*$_7$*-YFH1* cells treated with doxycycline. This is a late event that could be triggered by iron overload; this protein is known to be post-translationally regulated by metal levels (50). The experiment with the Δ*yfh*Δ*aft1* strain confirms this triggering, as preventing iron accumulation in the double mutant also prevents the decay in Smf2 levels. Inactivation of the cytosolic SOD isoenzyme was also observed previously in Δ*yfh1* cells (18). Again, this inactivation was described as the consequence of limited cofactor (in this case copper) availability. Copper is required for Fet3 activity, which is largely induced in Δ*yfh1* (51) and, as observed in this work, in *tetO-YFH1* mutants. Indeed, it has been described that activation of iron acquisition by the iron-responding factor Aft1 increases copper transport into membrane compartments, leading to copper-deprived cytosol (41). In summary, the results described here using the conditional *tetO-YFH1* mutants confirm the previous observations in Δ*yfh1* cells and provide an explanation for the origin of manganese deficiency in Yfh1-deficient cells.

The final conclusion of this study is that Yfh1 does not have an essential role in iron-sulfur biogenesis. Then what is the role of this mitochondrial protein? Our results can fit with two alternative hypotheses among those that have been formulated to explain frataxin function: the iron storage-detoxification hypothesis and the iron-sensing hypothesis. The first suggests that frataxin forms ferritin-like structures that store iron in an oxidized, nonreactive form (52). Lack of frataxin would lead to the formation of highly reactive iron forms that inactivate iron-sulfur-containing enzymes. The second one suggests that, rather than acting as the iron donor for iron-sulfur biogenesis, frataxin senses mitochondrial iron content and regulates the rate of iron-sulfur biogenesis (53). This second hypothesis would explain the interactions observed between frataxin and members of the iron-sulfur biosynthetic machinery (11–13), as well as its iron binding properties (54). Of course, one of the early consequences of losing either an iron storage protein or an iron-sensing protein could be the deregulation of iron metabolism, as observed in the present study. Also, any of these mitochondrial roles could explain why Yfh1 depletion leads not only to Aft1 activation but also to iron accumulation in the mitochondria. In this context, it is worth mentioning that the mitochondrial iron transporter Mrs4 is induced in Δ*yfh1* mutants (48), thus contributing to mitochondrial iron accumulation. In contrast, this induction is not observed in constitutively activated Aft1 mutants (the so-called Aft1-up) (55). This would indicate that such activation, in the absence of mitochondrial events, is not enough to explain the phenotype observed. The final clue needed to understand the primary role of frataxin may be obtained by deciphering the sequence of early events leading from Yfh1 depletion to Fet3 up-regulation.

Acknowledgments—We thank Jerry Kaplan (University of Utah) for critical review of the manuscript and Elaine M. Lilly for editorial assistance.

REFERENCES

1. Pandolfo, M., and Pastore, A. (2009) *J. Neurol.* **256,** Suppl. 1, 9–17
2. Campuzano, V., Montermini, L., Moltò, M. D., Pianese, L., Cossée, M., Cavalcanti, F., Monros, E., Rodius, F., Duclos, F., Monticelli, A., Zara, F., Cañizares, J., Koutnikova, H., Bidichandani, S. I., Gellera, C., Brice, A., Trouillas, P., De Michele, G., Filla, A., De Frutos, R., Palau, F., Patel, P. I., Di Donato, S., Mandel, J. L., Cocozza, S., Koenig, M., and Pandolfo, M. (1996) *Science* **271,** 1423–1427
3. Babcock, M., de Silva, D., Oaks, R., Davis-Kaplan, S., Jiralerspong, S., Montermini, L., Pandolfo, M., and Kaplan, J. (1997) *Science* **276,** 1709–1712
4. Koutnikova, H., Campuzano, V., Foury, F., Dollé, P., Cazzalini, O., and Koenig, M. (1997) *Nat. Genet.* **16,** 345–351
5. Wilson, R. B., and Roof, D. M. (1997) *Nat. Genet.* **16,** 352–357
6. Rötig, A., de Lonlay, P., Chretien, D., Foury, F., Koenig, M., Sidi, D., Munnich, A., and Rustin, P. (1997) *Nat. Genet.* **17,** 215–217
7. Foury, F. (1999) *FEBS Lett.* **456,** 281–284
8. Puccio, H., Simon, D., Cossée, M., Criqui-Filipe, P., Tiziano, F., Melki, J., Hindelang, C., Matyas, R., Rustin, P., and Koenig, M. (2001) *Nat. Genet.* **27,** 181–186
9. Raulfs, E. C., O'Carroll, I. P., Dos Santos, P. C., Unciuleac, M. C., and Dean, D. R. (2008) *Proc. Natl. Acad. Sci. U.S.A.* **105,** 8591–8596
10. Bandyopadhyay, S., Chandramouli, K., and Johnson, M. K. (2008) *Biochem. Soc. Trans.* **36,** 1112–1119
11. Gerber, J., Mühlenhoff, U., and Lill, R. (2003) *EMBO Rep.* **4,** 906–911
12. Wang, T., and Craig, E. A. (2008) *J. Biol. Chem.* **283,** 12674–12679
13. Gelling, C., Dawes, I. W., Richhardt, N., Lill, R., and Mühlenhoff, U. (2008) *Mol. Cell. Biol.* **28,** 1851–1861
14. Campanella, A., Isaya, G., O'Neill, H. A., Santambrogio, P., Cozzi, A., Arosio, P., and Levi, S. (2004) *Hum. Mol. Genet.* **13,** 2279–2288
15. Chen, O. S., and Kaplan, J. (2000) *J. Biol. Chem.* **275,** 7626–7632
16. Bulteau, A. L., Dancis, A., Gareil, M., Montagne, J. J., Camadro, J. M., and Lesuisse, E. (2007) *Free Radic. Biol. Med.* **42,** 1561–1570
17. Irazusta, V., Cabiscol, E., Reverter-Branchat, G., Ros, J., and Tamarit, J. (2006) *J. Biol. Chem.* **281,** 12227–12232
18. Irazusta, V., Obis, E., Moreno-Cermeno, A., Cabiscol, E., Ros, J., and Tamarit, J. (2009) *Free Radic. Biol. Med.*
19. Llorens, J. V., Navarro, J. A., Martínez-Sebastián, M. J., Baylies, M. K., Schneuwly, S., Botella, J. A., and Moltó, M. D. (2007) *FASEB J.* **21,** 333–344
20. Anderson, P. R., Kirby, K., Orr, W. C., Hilliker, A. J., and Phillips, J. P. (2008) *Proc. Natl. Acad. Sci. U.S.A.* **105,** 611–616
21. Mühlenhoff, U., Richhardt, N., Ristow, M., Kispal, G., and Lill, R. (2002) *Hum. Mol. Genet* **11,** 2025–2036
22. Chen, O. S., Hemenway, S., and Kaplan, J. (2002) *Proc. Natl. Acad. Sci. U.S.A.* **99,** 12321–12326
23. Lu, C., and Cortopassi, G. (2007) *Arch Biochem. Biophys.* **457,** 111–122
24. Wishart, J. A., Hayes, A., Wardleworth, L., Zhang, N., and Oliver, S. G. (2005) *Yeast* **22,** 565–569

25. Bellí, G., Garí, E., Aldea, M., and Herrero, E. (1998) *Yeast* **14,** 1127–1138
26. Janke, C., Magiera, M. M., Rathfelder, N., Taxis, C., Reber, S., Maekawa, H., Moreno-Borchart, A., Doenges, G., Schwob, E., Schiebel, E., and Knop, M. (2004) *Yeast* **21,** 947–962
27. Garí, E., Piedrafita, L., Aldea, M., and Herrero, E. (1997) *Yeast* **13,** 837–848
28. Tamarit, J., Irazusta, V., Moreno-Cermeño, A., and Ros, J. (2006) *Anal. Biochem.* **351,** 149–151
29. Robinson, J., Brent, L., Sumegi, B., and Srerre, P. (1987) in *Mitochondria: A Practical Approach* (Darley-Usmar, V. M., Rickwood, D., and Wilson, M. T., eds) pp. 153–179, IRL Press, Oxford, United Kingdom
30. Manchenko, G. P. (1994) *Handbook of Detection of Enzymes on Electrophoretic Gels*, p. 98, CRC Press LLC, Boca Raton, FL
31. Reverter-Branchat, G., Cabiscol, E., Tamarit, J., Sorolla, M. A., Angeles de la Torre, M., and Ros, J. (2007) *Microbiology* **153,** 3667–3676
32. Bellí, G., Garí, E., Piedrafita, L., Aldea, M., and Herrero, E. (1998) *Nucleic Acids Res.* **26,** 942–947
33. Cabiscol, E., Piulats, E., Echave, P., Herrero, E., and Ros, J. (2000) *J. Biol. Chem.* **275,** 27393–27398
34. Li, L., and Kaplan, J. (2001) *J. Biol. Chem.* **276,** 5036–5043
35. Guarente, L. (1983) *Methods Enzymol.* **101,** 181–191
36. Pfaffl, M. W. (2006) in *Real-time PCR* (Dorak, T., ed) pp 63–82, Taylor & Francis Group, New York
37. Swanson, W. H., and Clifton, C. E. (1948) *J. Bacteriol.* **56,** 115–124
38. Díaz-Ruiz, R., Avéret, N., Araiza, D., Pinson, B., Uribe-Carvajal, S., Devin, A., and Rigoulet, M. (2008) *J. Biol. Chem.* **283,** 26948–26955
39. Kaplan, J. (1999) *Proc. Natl. Acad. Sci. U.S.A.* **96,** 10948–10949
40. Kumánovics, A., Chen, O. S., Li, L., Bagley, D., Adkins, E. M., Lin, H., Dingra, N. N., Outten, C. E., Keller, G., Winge, D., Ward, D. M., and Kaplan, J. (2008) *J. Biol. Chem.* **283,** 10276–10286
41. Philpott, C. C., and Protchenko, O. (2008) *Eukaryot. Cell* **7,** 20–27
42. Condò, I., Malisan, F., Guccini, I., Serio, D., Rufini, A., and Testi, R. (2010) *Hum. Mol. Genet.* **19,** 1221–1229
43. Schmucker, S., Argentini, M., Carelle-Calmels, N., Martelli, A., and Puccio, H. (2008) *Hum. Mol. Genet.* **17,** 3521–3531
44. Irazusta, V., Moreno-Cermeño, A., Cabiscol, E., Ros, J., and Tamarit, J. (2008) *Free Radic. Biol. Med.* **44,** 1712–1723
45. Rodríguez-Manzaneque, M. T., Tamarit, J., Bellí, G., Ros, J., and Herrero, E. (2002) *Mol. Biol. Cell* **13,** 1109–1121
46. Luk, E. E., and Culotta, V. C. (2001) *J. Biol. Chem.* **276,** 47556–47562
47. Portnoy, M. E., Liu, X. F., and Culotta, V. C. (2000) *Mol. Cell. Biol.* **20,** 7893–7902
48. Foury, F., and Roganti, T. (2002) *J. Biol. Chem.* **277,** 24475–24483
49. Wallace, M. A., Liou, L. L., Martins, J., Clement, M. H., Bailey, S., Longo, V. D., Valentine, J. S., and Gralla, E. B. (2004) *J. Biol. Chem.* **279,** 32055–32062
50. Reddi, A. R., Jensen, L. T., and Culotta, V. C. (2009) *Chem. Rev.* **109,** 4722–4732
51. Foury, F., and Talibi, D. (2001) *J. Biol. Chem.* **276,** 7762–7768
52. Schagerlöf, U., Elmlund, H., Gakh, O., Nordlund, G., Hebert, H., Lindahl, M., Isaya, G., and Al-Karadaghi, S. (2008) *Biochemistry* **47,** 4948–4954
53. Adinolfi, S., Iannuzzi, C., Prischi, F., Pastore, C., Iametti, S., Martin, S. R., Bonomi, F., and Pastore, A. (2009) *Nat. Struct. Mol. Biol.* **16,** 390–396
54. Cook, J. D., Bencze, K. Z., Jankovic, A. D., Crater, A. K., Busch, C. N., Bradley, P. B., Stemmler, A. J., Spaller, M. R., and Stemmler, T. L. (2006) *Biochemistry* **45,** 7767–7777
55. Shakoury-Elizeh, M., Tiedeman, J., Rashford, J., Ferea, T., Demeter, J., Garcia, E., Rolfes, R., Brown, P. O., Botstein, D., and Philpott, C. C. (2004) *Mol. Biol. Cell* **15,** 1233–1243
56. Molina-Navarro, M. M., Castells-Roca, L., Bellí, G., García-Martínez, J., Marín-Navarro, J., Moreno, J., Pérez-Ortín, J. E., and Herrero, E. (2008) *J. Biol. Chem.* **283,** 17908–17918

Metabolism:

Frataxin Depletion in Yeast Triggers Up-regulation of Iron Transport Systems before Affecting Iron-Sulfur Enzyme Activities

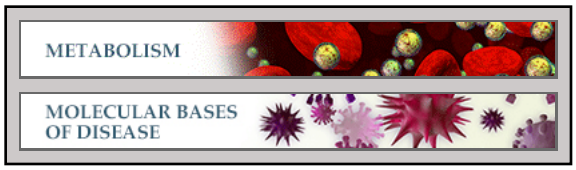

Armando Moreno-Cermeño, Èlia Obis, Gemma Bellí, Elisa Cabiscol, Joaquim Ros and Jordi Tamarit

J. Biol. Chem. 2010, 285:41653-41664.
doi: 10.1074/jbc.M110.149443 originally published online October 18, 2010
